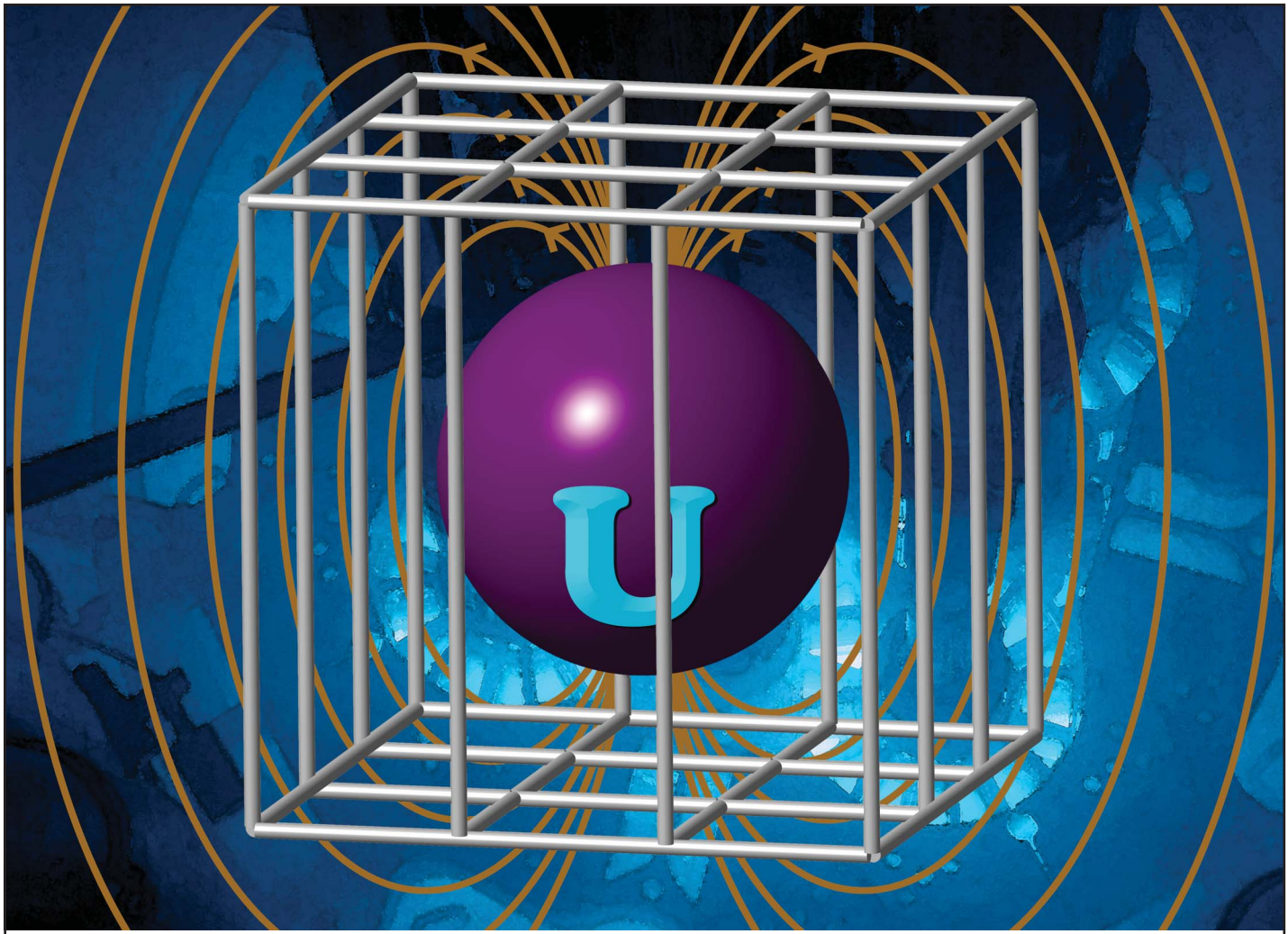

Showcasing research from the laboratory of Prof. Eugenio Coronado, Institute of Molecular Science, University of Valencia, Spain.

Modeling the properties of uranium-based single ion magnets

In the right coordination environment, U(III) seems to be an apt choice for the preparation of single-molecule magnets, while U(IV) offers an unmatched potential for molecular spin qubits.

As featured in:

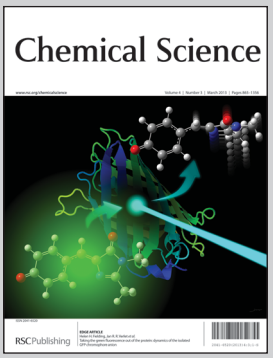

See Eugenio Coronado, Alejandro Gaita-Ariño *et al.*, *Chem. Sci.*, 2013, **4**, 938.

RSC Publishing

www.rsc.org/chemicalscience

Registered Charity Number 207890

Chemical Science

RSC Publishing

EDGE ARTICLE

Modeling the properties of uranium-based single ion magnets†

Cite this: *Chem. Sci.*, 2013, **4**, 938

José J. Baldoví, Salvador Cardona-Serra, Juan M. Clemente-Juan, Eugenio Coronado* and Alejandro Gaita-Ariño*

Received 10th September 2012
Accepted 21st November 2012

DOI: 10.1039/c2sc21490c

www.rsc.org/chemicalscience

We analyze the magnetic behavior of the five uranium-based SIMs reported in the literature. By combining a corrected crystal field model with the magnetic experimental data, we obtain the lowest-lying magnetic levels and the associated wave functions of the nanomagnets, which are found to be compatible with the observed SMM behavior. Additionally, this approach has allowed us to propose some geometrical considerations and practical advice for experimentalists aiming for the rational design of SIMs and spin qubits based on uranium.

Published on 22 November 2012 on http://pubs.rsc.org | doi:10.1039/C2SC21490C
Downloaded by Technische Universiteit Delft on 05 February 2013

Introduction

Owing to their rich physical behavior, including new quantum phenomena, mononuclear complexes formed by an anisotropic metal—usually a lanthanoid ion—with single-molecule magnetic (SMM) behavior have become a hot topic in molecular magnetism.[1,2] Such mononuclear SMMs, usually known as single ion magnets (SIMs), are promising candidates in molecular spintronics[3–6] and quantum computing.[7,8] The first example of these molecular nanomagnets was reported by Ishikawa *et al.* in 2003 in a family of complexes of general formula $[Ln(Pc)_2]^-$, with a 'double-decker' structure, where a lanthanoid ion is sandwiched between two phthalocyanine moieties.[9] That pioneer work inspired the design of other derivatives[10–12] and nowadays, the concept of SIMs has been extended to a large number of families of mononuclear lanthanoid complexes.[13] In contrast with polynuclear SMMs, where exchange interactions drive their properties, in the mononuclear lanthanoid complexes these properties are directly related with the crystal field created by the surrounding ligands. Thus, in a given crystal field the ground magnetic state of the complex, characterized by the total angular momentum, J, splits into $\pm M_J$ sublevels. In some cases this leads to a J-splitting in which the levels with the higher $|M_J|$ values are stabilized with respect to the levels with the lower $|M_J|$ values. In these cases a barrier that explains the superparamagnetic blocking observed in the SIMs appears. At the same time, the magnetic behavior of these systems is dominated by quantum effects at low temperature, which are strongly affected not only by the structural and electronic features of the molecule, but also by their surroundings (spin bath and phonon bath), making their spin dynamics a complex and very poorly understood problem.[14] Still, these processes can be at the origin of important physical phenomena, such as the field-induced multiple relaxation processes[15,16] and the giant field dependence of the relaxation time.[17]

Currently, obtaining new molecules with larger energy barriers and the understanding of the quantum tunneling processes are the two major challenges in this field. Regarding the first point, actinoids are attracting a growing attention. Thus, due to higher spin-orbit coupling, larger magneto-crystalline anisotropy, and enhanced covalence, they have been defined as better candidates to provide SIMs than lanthanoids, as the J-ground state splitting caused by the CF is expected to be higher.[18,19] Those features are related to the 5f electrons, which are more extended than the 4f electrons on lanthanoids and interact more with the electron density of the ligands.

Still, only a handful of examples of SIMs based on actinoids have been reported so far. The Long group published the first two examples of uranium-based SIMs. The first one was measured in 2009 in a diphenylbis(pyrazolborate) uranium(III) complex formulated as $U(Ph_2BPz_2)_3$ (**1**),[20] previously isolated in 1999 by I. Santos *et al.*[21] One year later, a second example of the same family was reported in the dihydrobis(pyrazolborate) derivative $U(H_2BPz_2)_3$ (**2**).[22] Recently, the list has been extended with the discovery of the SMM behavior in the complex UTp_3 (**3**) (Tp^- = trispyrazolylborate).[23] Independently, M. Almeida *et al.* have reported two further examples closely related of U(III) SIMs: the cationic complex $[U(TpMe_2)_2(bipy)]^+$ (**4**), where $TpMe_2$ = hydrotris(3,5-dimethylpyrazolyl),[24] and its precursor $[U(TpMe_2)_2I]$ (**5**),[25] first prepared and characterized by Takats *et al.*[26] Other actinoid-based SMMs that are not treated in this study are a mononuclear complex based on neptunium, $[Np(COT)_2]$ ($COT = C_8H_8^{2-}$),[27] and two polynuclear complexes: the trimetallic cluster $\{Np^{VI}O_2Cl_2\}\{Np^{V}O_2Cl(thf)_3\}_2$,[28] also

Instituto de Ciencia Molecular (ICMol), Universidad de Valencia, C/Catedrático José Beltrán, 2, E-46980 Paterna, Spain. E-mail: eugenio.coronado@uv.es; alejandro.gaita@uv.es

† Electronic supplementary information (ESI) available. See DOI: 10.1039/c2sc21490c

This journal is © The Royal Society of Chemistry 2013

Published on 22 November 2012 on http://pubs.rsc.org | doi:10.1039/C2SC21490C
Downloaded by Technische Universiteit Delft on 05 February 2013

known as Np_3, and the polynuclear U(III) complex of formula $[(U(BIPM^{TMS}H)(I))_2(\mu\text{-}\eta^6\text{:}\ \eta^6\text{-}C_6H_5CH_3)]$, where $BIPM^{TMS} = C(PPh_2NSiMe_3)_2$.[29]

In this paper, we are going to focus on compounds **1** to **5**. In all these cases the coordination environment around U(III) is formed mostly by nitrogen donor atoms from pyrazole rings. The interpretation of the magnetism of these compounds is still an open question. The main objective of this paper is to rationalize the magnetic behavior of these $5f^3$ complexes by getting a first estimation of the splitting of the U(III) *J*-ground state caused by the ligand field. A second objective will be that of predicting which are the most suitable coordination geometries that can provide uranium-based SIMs.

Theoretical approach

Our calculations are primarily based on an effective crystal field (CF) Hamiltonian that considers a point-charge electrostatic (PCE) model, which has been previously proven to be useful for the rationalization of the magnetic properties of lanthanoid SIMs[30] and is implemented in the software package SIMPRE.[31] The starting point is the set of atomic coordinates of the target compound that can in principle be idealized in order to obtain the main CF parameters. These calculations were already used in the sixties to study the CF terms for the cubic system UO_2.[32] Still, such a model only provides a crude approximation of the reality. In fact, recent experimental studies have shown that the point charge model heavily underestimates the high-degree terms, as it does not take into account overlap and covalency effects.[33] To improve this limitation, instead of assuming a charge of $Z_i = 1$ that is centered on the nitrogen atom, we use effective point charges. Because the lone pairs of the N donor atoms in these complexes are pointing almost directly toward the uranium nucleus, we can parameterize them through a radial contraction D_r and a charge Z_i, *i.e.* a Radial Effective Charge (REC) model, as we would normally do for spherical ligands.[34] As all the compounds under study are based on ligands that coordinate to the uranium through pyrazole rings, we have reproduced the properties of the five complexes allowing only small variations around the average values for D_r and Z_i. These effective coordinates are used to obtain an estimation of the CF parameters, A_k^q and B_k^q. Then, these parameters are introduced in a CF Hamiltonian, which has the general form:

$$\widehat{H}_{cf}(J) = \sum_{k=2,4,6}\sum_{q=-k}^{k} B_k^q O_k^q = \sum_{k=2,4,6}\sum_{q=-k}^{k} a_k(1-\sigma_k)A_k^q\langle r^k\rangle O_k^q \quad (1)$$

where k is the order (also called rank or degree) of the Stevens operator equivalents O_k^q, and q is the operator range that varies between k and $-k$, a_k are the α, β and γ Stevens coefficients[35] for $k = 2$, 4, 6, respectively, σ_k are the Sternheimer shielding parameters[36] of the 5f electronic shell and $\langle r^k\rangle$ are the expectation values of the radial factor r^k.[37] α, β and γ are tabulated and depend on the number of f-electrons. For U(III) ($5f^3$ ion) such parameters are:

$\alpha = -6.42753 \times 10^{-3}$, $\beta = -2.9117 \times 10^{-4}$ and $\gamma = -3.7988 \times 10^{-5}$, and the shielding parameters are $\sigma_2 = 0.83$, $\sigma_4 = 0.026$ and $\sigma_6 = -0.039$.

We need to remember that the negative sign of α translates positive ${A_2}^0$ into negative ${B_2}^0$ *i.e.* an easy-axis anisotropy.

The A_k^q CF parameters may be calculated by the following expression:

$$A_k^q = \frac{4\pi}{2k+1} c_{kq}(-1)^q \sum_{i=1}^{N} \frac{Z_i e^2 Y_{k-q}(\theta_i,\varphi_i)}{R_i^{k+1}} \quad (2)$$

R_i, θ_i and φ_i are the effective polar coordinates of the point charge and Z_i is the effective point charge, associated to the *i*-th ligand with the lanthanoid at the origin; e is the electron charge and c_{kq} is a tabulated numerical factor that relates spherical harmonics Y_{k-q} and Stevens operator equivalents.

For each compound, we refine this Hamiltonian by means of a fit to the magnetic susceptibility curve. In addition to the CF parameters, we include one term accounting for potentially miscorrected temperature independent paramagnetism (or diamagnetism), plus a scaling factor F. In the fitting procedures, we define the error R as:

$$R = \frac{\sum_N \left[\chi_{exp}T - \chi_{theo}T\right]^2}{N\sum_N \left[\chi_{exp}T\right]^2} \quad (3)$$

where $\chi_{exp}T$ and $\chi_{theo}T$ are experimental and theoretical values, respectively, and N is the number of points.

Notice that we have assumed the Russell–Saunders approximation, which considers the ground J spin-orbit state well isolated from excited ones. This approach is very useful to study lanthanoid SIMs, where the spin-orbit (L-S) coupling is about an order of magnitude stronger than the ligand field. However, this situation differs for actinoids, because the 5f orbitals are more diffuse and both spin-orbit coupling and ligand field are more intense. Intermediate coupling calculations have shown that for $5f^2$, $5f^3$ and $5f^4$ configurations the Russell–Saunders state makes up around 80% of the true ground state.[38] This should be compared with 94% in the case of Er^{3+}, and with the worst scenario for other actinoids, Am^{3+} (44.9%). This means that for the U(III) this model is reasonable as it accounts for a 84.1% of the ground state ($^4I_{9/2}$). For the χT product fitting we have used a corrected Landee g_J factor taking into account the first J excited state ($^2H_{9/2}$), *i.e.* $g_J = 0.84\ (8/11) + 0.16\ (2/3)$. Notice that employing the Russell–Saunders approximation would be slightly worse for U^{4+} as it represents a 77.5%.[39] In general, such approach can be used at least as a good starting point for understanding actinoid single-ion anisotropy.[40]

Results and discussion

Here we will focus on the five U(III) mononuclear complexes that have been shown to behave as SIMs so far. In the first four complexes the uranium cation is coordinated only to nitrogen atoms and in complex **5** it is also bonded to an iodide anion. As for the lanthanoid SIMs, the SMM behavior of these actinoid SIMs is expected to depend on the structure of the low-lying

Published on 22 November 2012 on http://pubs.rsc.org | doi:10.1039/C2SC21490C
Downloaded by Technische Universiteit Delft on 05 February 2013

energy levels and the associated wave functions. Thus, a detailed knowledge of these features is crucial to understand the SMM behavior of these systems. In particular, this information is very useful to predict which geometries are more suited to present a superparamagnetic barrier and a blocking of the magnetic moment. Here we extract this information by using a Radial Effective Charge (REC) model to obtain the parameters of the crystal field Hamiltonian.[34] We do this by fitting the experimental properties—*e.g.* magnetic susceptibility from the effective coordinates and charges, obtaining the full set of CF parameters, the energy level scheme and the associated wave functions.

$U(Ph_2BPz_2)_3$ and $U(H_2BPz_2)_3$

Compounds **1** and **2** are structurally very similar and thus will be discussed together. Both are U(III) complexes coordinated by three bis(pyrazolyl)borate ligands (see Fig. 1). The difference between them lies in the ligands which are diphenylbis(pyrazolborate) in the first case, compound **1**, and dihydrobis(pyrazolborate) in the second one, **2**. This produces important differences in the crystal structure but only minor distortions in the coordination sphere. In both cases the environment of the U(III) center is trigonal prismatic with an approximate D_{3h} symmetry. To quantify the deviation of both real structures to the ideal trigonal prism, we have used the SHAPE software,[41] where a continuous shape measure S_P is mathematically defined in a way that is independent of the size of the system. By definition, the resulting value of S_P is zero when the real coordinates of the metal site (problem structure, P) show exactly the desired ideal shape, and increases with the degree of distortion of the structure. Values below 0.1 represent chemically insignificant distortions in the structure. Values larger than 3 mean important distortions, with the highest values commonly encountered being in the order of 40. Using the corresponding idealized D_{3h} trigonal prisms as target structures, one obtains values of $S_P = 0.268$ for compound **1** and $S_P = 0.260$ for **2**. All other hexacoordinated target structures result in values of $S_P > 10$, supporting the view that these structures are slightly distorted trigonal prisms. Therefore, we have referred our coordinate system aligned with the main symmetry axis of the trigonal prism in both cases.

Given the coordination environment of compounds **1** and **2**, a clear magnetic easy-axis is expected for both cases, but because of those deviations from ideality, the Hamiltonian corresponding to the REC model includes all possible terms of eqn (1), providing a more realistic description of the system. A fitting of the magnetic susceptibility data of **1** and **2** (available from ref. 20 and 22) from 20 to 300 K allows us to determine the radial displacement, D_r, and the effective charge, Z_i, that provide the whole set of CF parameters, related to the original atomic coordinates, which explain the measured χT product. Note that the χT product under 20 K is not considered for the fitting due to the presence of dipolar interactions at lower temperatures, as evidenced by the drastic variation of the susceptibility between diluted and concentrated samples in compound **2**.[42] A satisfactory fitting of the χT product is obtained for a $D_r = 1.30$ Å and $Z_i = 0.0247$ in compound **1**, while $D_r = 1.40$ Å and $Z_i = 0.0203$ in **2**. In both cases we use the same corrections, TIP $= -1.5 \times 10^{-3}$ emu mol^{-1} and $F = 0.95$.

As can be seen in Fig. 2, the agreement between the model and the experimental data is excellent from 20 to 300 K, where

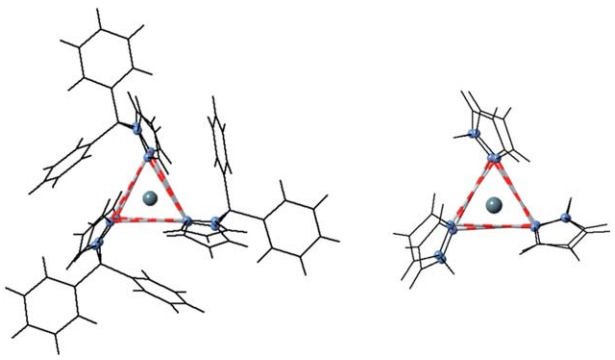

Fig. 1 Eclipsed views of the molecular structure of $U(Ph_2BPz_2)_3$ (**1**, left) and $U(H_2BPz_2)_3$ (**2**, right); the corresponding trigonal prismatic coordination spheres are highlighted.

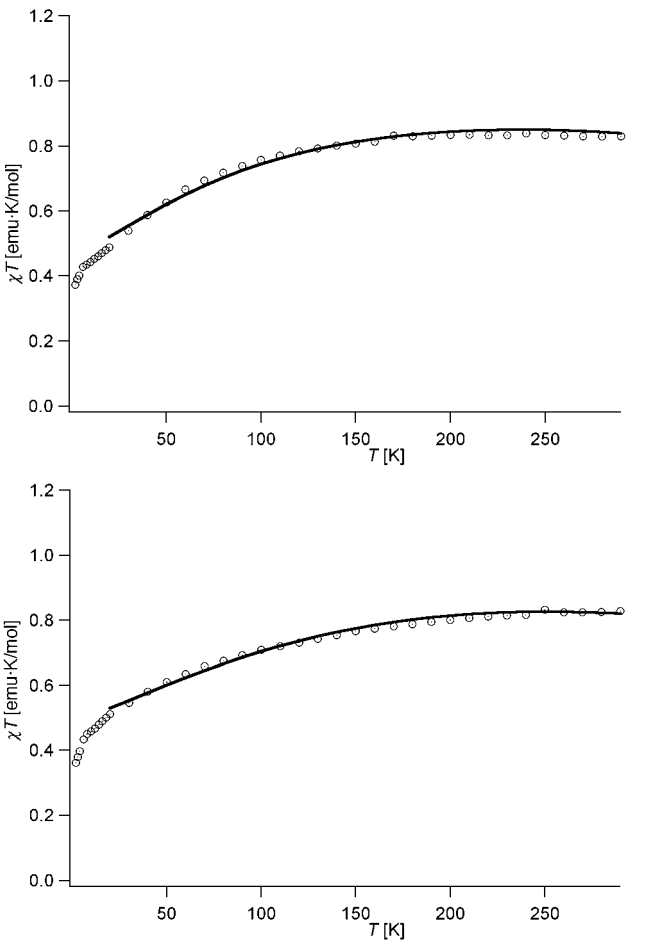

Fig. 2 χT product for complex **1** (up) and **2** (down). Open circles: experimental data; solid line: theoretical fit from 20 to 300 K.

This journal is © The Royal Society of Chemistry 2013

Published on 22 November 2012 on http://pubs.rsc.org | doi:10.1039/C2SC21490C
Downloaded by Technische Universiteit Delft on 05 February 2013

dipolar interactions are negligible. The resulting full set of CF parameters is available as ESI (Tables S1 and S2†) and the key points that are worth discussing are: (a) among the diagonal parameters, A_4^0 dominates, as expected considering the polar angle of the coordinating nitrogen atoms (Fig. 3), and (b) among the extradiagonal parameters, A_6^6 has a prominent role, as the coordination environment corresponds to a trigonal prism. The deviations from ideality are mostly reflected in the high values of A_6^5 in complex **1**, and the lower but also high values of A_6^5 and A_4^3in complex **2**. Note that, because of the location of the boron-bound hydrogens, a significant amount of electron density may be found closer to the equatorial plane in compound **2**. It might then be described as triaugmented trigonal prismatic. As there are not enough data to quantify this effect, qualitatively it would lead to a smaller value of A_2^0.

The energy level scheme for both compounds is depicted in Fig. 4. As a consequence of the symmetry-allowed extradiagonal parameter, A_6^6, we find that the major mixing in the wave function occurs between M_J values that differ by six units. In **1** the ground level is a doublet mainly described by the wave functions: 0.79 |+ 5/2> + 0.17 |− 7/2> and 0.79 |− 5/2> + 0.17 |+ 7/2>. The REC model also allows to estimating the contamination of the ground state wave function by minor M_J components, which would not be allowed by the major extradiagonal terms. The sum of all such terms is less than 4% for **1**. The first excited level lies at about $\Delta = 190$ cm^{-1} with a wave function mixed between $\pm 3/2$ and $\mp 3/2$ (66%) and 18% of $\mp 9/2$. The description of the lowest levels of (**1**) is perfectly compatible with the reported SMM behavior of the complex, because there is not direct mixing between $+M_J$ and $-M_J$ in the ground doublet.

For complex **2**, and always according to this effective description, the ground doublet is again a mixture involving 0.68 |+ 5/2> + 0.24 |− 7/2> and 0.68 |− 5/2> + 0.24 |+ 7/2>. The sum of all terms which are not allowed in an ideal approximation of the coordination environment reaches 8%, which accounts for the small deviations from ideality, which in this case is parameterized by a large A_4^3 parameter. Still, this is compatible with a SMM behavior because there is no direct mixing between $+M_J$ and $-M_J$ in the ground state. The first excited state is located at 230 cm^{-1}, and again, like in **1**, it is a doublet mixed between $\pm 3/2$ and $\mp 3/2$ (52%) and a 32% of $\mp 9/2$.

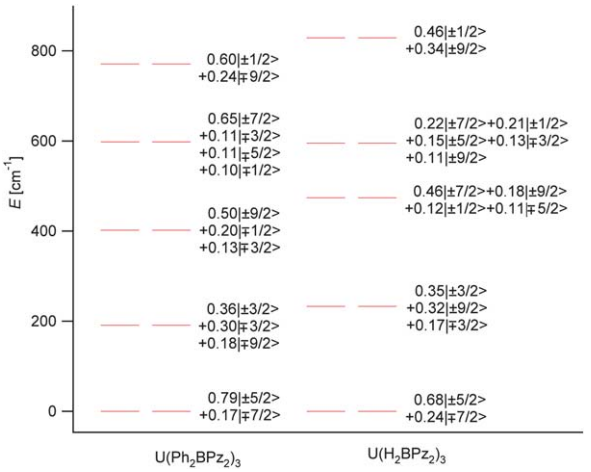

Fig. 4 Energy level scheme and main contributions to the wave functions for complexes **1** and **2**.

Finally, it is tempting to establish a correspondence between these energy gaps (190 cm^{-1} and 230 cm^{-1} for **1** and **2**), and the effective barriers, U_{eff} (20 cm^{-1} and 8 cm^{-1} respectively). As we notice there is not any relationship between these values, emphasizing that this kind of models are unable to predict the magnitude of this gap. Probably the relaxation processes involve virtual states that are not accounted for by this energy scheme.

UTp_3

Complex **3** is formed by a uranium(III) ion surrounded by three trispyrazolylborate (Tp^-) ligands. The magnetic ion is directly bonded to nine pyrazole rings in a crystallographically exact D_{3h} tricapped trigonal prism coordination environment (Fig. 5).

In this case, an experimental energy level scheme is available, as it was determined spectroscopically by Apostolidis *et al.*[43] Thus, we used these higher-quality data to parameterize the system. Again, we employed the REC model because the lone pairs point almost toward the metal site. As we are interested in the magnetic properties around or below room

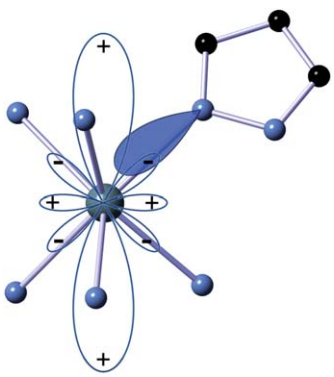

Fig. 3 Orientation and electronic distribution of the lone pair in compound **1** and representation of the shape of the spherical harmonic Y_4^0.

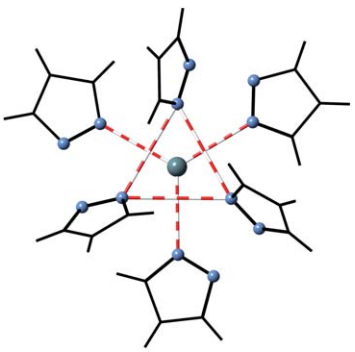

Fig. 5 Eclipsed view of the tricapped trigonal prismatic coordination structure of $U(Tp)_3$; the full trispyrazolylborate ligands are omitted for clarity.

Published on 22 November 2012 on http://pubs.rsc.org | doi:10.1039/C2SC21490C
Downloaded by Technische Universiteit Delft on 05 February 2013

temperature, the fit considers only the levels below 600 cm^{-1} in order to provide a better reproduction of these levels. A satisfactory fitting of such levels is obtained for a $D_r = 1.35$ Å and $Z_i = 0.0223$ (Fig. 6). These parameters are very similar to the ones we obtained for compounds **1** and **2**, as expected owing to the very similar character of the ligands, which results in a similar electrostatic effect of the nitrogen donor atoms over the uranium cation.

Due to the high symmetry of this example, the crystal field splitting might be described by the simplified CF Hamiltonian (eqn (4)):

$$H_{CF} = \sum_{k=2,4,6} a_k(1-\sigma_k)A_k{}^0\langle r^k\rangle O_k{}^0 + \gamma(1-\sigma_6)A_6{}^6\langle r^6\rangle O_6{}^6 \quad (4)$$

As seen in complexes **1** and **2**, the diagonal $A_4{}^0$ CF parameter dominates the splitting and the extradiagonal parameter $A_6{}^6$ is in the same order of magnitude as calculated for compounds **1** and **2**. In particular, as a consequence of the symmetry-allowed $A_6{}^6$, one can understand that the mixing in the wave function occurs between M_J values that differ by six units *i.e.* between $M_J = \pm 7/2$ and $M_J = \mp 5/2$, or between $M_J = \pm 9/2$ and $M_J = \mp 3/2$.

Finally, the experimental susceptibility curve of complex **3** is closely reproduced (Fig. 7) using the previously obtained set of CF parameters (Table S3†). A TIP correction of 10^{-4} emu mol^{-1} and a scaling factor F of 0.95 have been applied to our theoretical data.

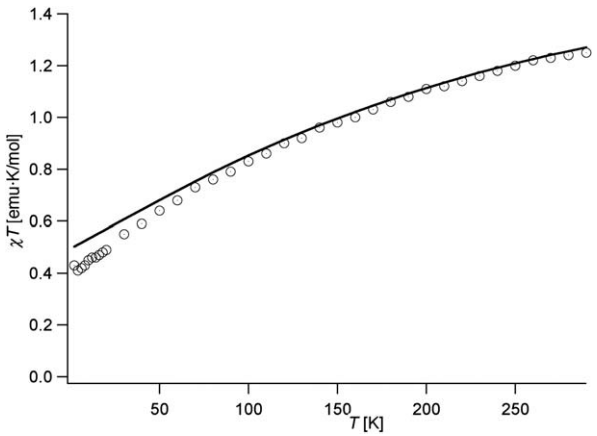

Fig. 7 χT product for complex **3**. Open circles: experimental data; solid line: theoretical estimation using the fit for the energy levels (Fig. 6).

$[U(Tp^{Me2})_2(bipy)]^+$ and $[U(Tp^{Me2})_2I]$

Structures of complexes **4** and **5** are farther from ideality (Fig. 8) compared with the first three compounds. In **4**, the first coordination sphere can be viewed either as a very distorted square antiprism or, more accurately, as a scheelite-like triangular dodecahedron that has been twisted by 45 degrees. Using SHAPE software, the continuous shape measure with a triangular dodecahedron as target structure results in $S_P = 1.344$, while when the target structure is a square antiprism, $S_P = 3.109$. As explained before, this means that in both cases there are chemically significant deviations from the ideal structure, which are important in the case of the square antiprism ($S_P > 3$). The same approach for compound **5** yields $S_P = 2.839$ for a pentagonal bipyramid (D_{5h}) as a target structure, and even higher values for any other possibility of coordination index equals to 7, meaning that no simplified description of the structure is really adequate in this case. In fact, both complexes deviate enough from the ideal symmetries that there is not a simple relation between their coordination environment and the obtained CF parameters (Tables S4 and S5†). Here it is important to remember that, while the physical properties are obviously independent of our choice of the coordinate axis criterion, both the CF parameters and the coefficients of the

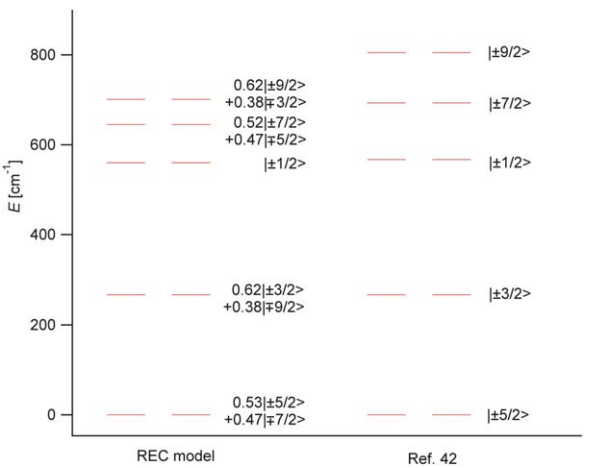

Fig. 6 Energy level scheme for complex **3** determined by the REC model (left) and in ref. 43 (right).

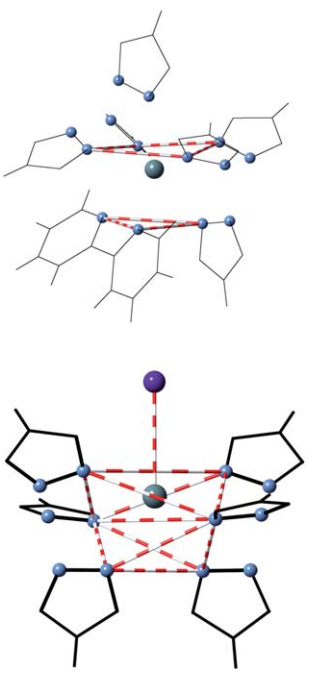

Fig. 8 Molecular structure of $[U(Tp^{Me2})_2(bipy)]$ (**4**, up) and $[U(Tp^{Me2})_2I]$ (**5**, down).

This journal is © The Royal Society of Chemistry 2013

Published on 22 November 2012 on http://pubs.rsc.org | doi:10.1039/C2SC21490C
Downloaded by Technische Universiteit Delft on 05 February 2013

wave function are very much dependent of this choice, which is to some extent arbitrary. For very distorted systems, this dependence is often in non-trivial.

The procedure discussed above was repeated for the χT data of compounds **4** and **5**. Satisfactory fits could be obtained with REC parameters for the pyrazole-based ligands that are within the range of those obtained for complexes **1**, **2** and **3** (see Table 1). Compared with the fitting procedures for such compounds, there are more free parameters for complexes **4** and **5**, because of the additional ligands (bipyridine in compound **4** and iodide in **5**). This results in a slight overparameterization, where minor improvements can be found in the low-temperature behavior at the cost of an unrealistic increase in the crystal field splitting. As a result, we had to include an upper limit of 1000 cm^{-1} in the total CF splitting as an additional condition. In complex **4** the bipyridine ligand effect was reproduced with $D_r = 1.25$ Å and $Z_i = 0.133$ for the two coordinated nitrogen atoms, and the contribution of the iodine anion in **5** was parameterized with $D_r = 1.88$ Å and $Z_i = 0.0843$.

The result of the fitting is represented in Fig. 9. Note that a significant scaling factor $F = 0.65$ was needed to correlate our theoretical χT values with the experimental ones for complex **4**, a fact that should be taken into consideration when reading the corresponding set of energy levels and wave functions. This disagreement between theory and experiment was already noticed by the authors, which needed a similar scaling factor for making the experimental χT curve compatible with the *ab initio* SO-CASPT2 calculations.[25] The origin of this disagreement is unclear but might be due to the experiment. In fact, it does not appear in the closely related system **5** for which the scaling factor is more realistic ($F = 0.92$) and compatible with the experimental data.

The resulting energy level schemes and the associated wave functions are depicted in Fig. 10. It is important to remark that there is no direct mixing of $+M_J$ and $-M_J$ in the ground state of either compound, a compatible description with the reported SMM behavior. The ground state doublet is formed by a combination of 0.31 |+ 3/2> + 0.27 |− 5/2> + 0.15 |− 7/2> and 0.31 |− 3/2> + 0.27 |+ 5/2> + 0.15 |+ 7/2> in **4**, whereas it is composed by 0.35 |+ 9/2> + 0.34 |+ 5/2> + 0.28 |− 3/2> and 0.35 |− 9/2> + 0.34 |− 5/2> + 0.28 |+ 3/2> in **5**. The resulting gaps with the first excited levels are 110 cm^{-1} and 136 cm^{-1}, for **4** and **5** respectively, which are in the same order of magnitude as those reported by Almeida *et al.* (146 cm^{-1} and 138 cm^{-1}).[25] As we discussed before for compounds **1** and **2**, these barriers that depend on the electronic structure are higher than the effective energy barriers reported (U_{eff} (**4**) = 21.0 cm^{-1} and U_{eff} (**5**) = 18.2 cm^{-1}).

Table 1 summarizes the Radial Effective Charge parameters for the pyrazole ligand resulting from all χT fittings in the present work. Very similar values for the radial displacements

Table 1 Radial displacement and effective charge of pyrazole nitrogen and fitting parameters for compounds **1** to **5**

	D_r (Å)	Z_i	TIP (emu mol^{-1})	F	R
1	1.30	0.0247	-1.5×10^{-3}	0.95	4.71×10^{-3}
2	1.40	0.0203	-1.5×10^{-3}	0.95	8.65×10^{-3}
3	1.35	0.0223	1.0×10^{-4}	0.95	1.00×10^{-2}
4	1.40	0.0154	1.0×10^{-4}	0.65	3.34×10^{-5}
5	1.35	0.0293	-3.5×10^{-4}	0.92	1.36×10^{-3}

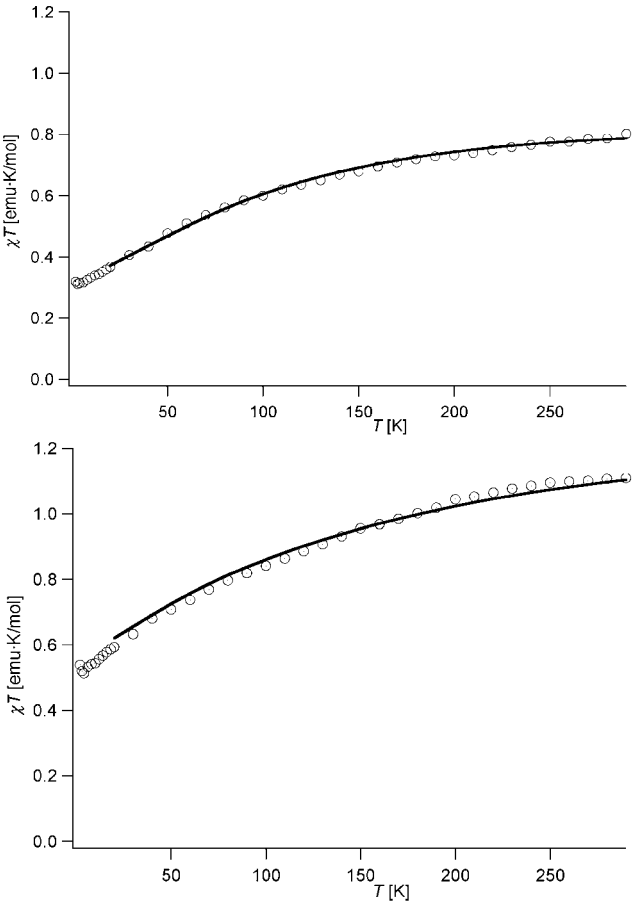

Fig. 9 χT product for complex **4** (up) and **5** (down). Open circles: experimental data; solid line: theoretical fit from 20 to 300 K.

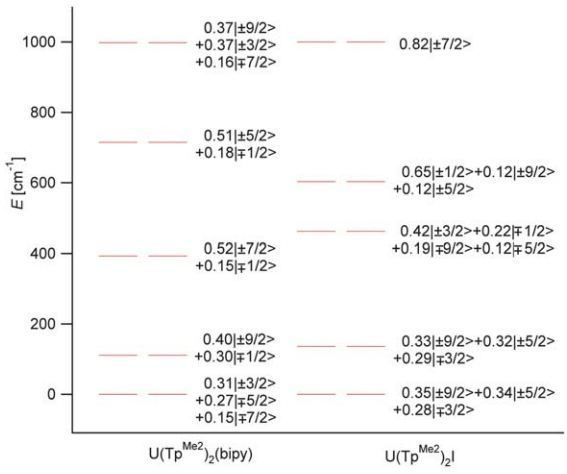

Fig. 10 Energy level scheme and main contributions to the wave functions for complexes **4** and **5**.

Published on 22 November 2012 on http://pubs.rsc.org | doi:10.1039/C2SC21490C
Downloaded by Technische Universiteit Delft on 05 February 2013

and the same order of magnitude of the effective charge result in adequate fits in all cases. The corrections for either TIP or diamagnetic contribution are close to zero in every case. The scaling factors are close to unity, except in the case of compound **4**, as discussed above.

In view of the previous considerations, this result can be seen as an indication of the adequacy of the REC model to estimate the crystal field Hamiltonian in Uranium complexes, at least when simultaneous fittings are possible for a family of chemically related complexes. More generally, it means that the theoretical tools developed for the study of lanthanoid SIMs within the Russell-Saunders approximation can also be employed to study uranium SIMs.

Rational design of uranium-based SIMs and spin qubits

There is a number of considerations to take into account when aiming a mononuclear uranium complex to display SMM properties. A number of different symmetries are possible for both of the most common oxidation states, U(III) and U(IV). When analyzing them, our guiding principle will be the cancellation for symmetry reasons of any direct mixing within the ground doublet. If possible, we will also avoid potential mixing at $\Delta M_J = 1$ as this will make the system more resilient to stray perpendicular magnetic fields or phonons.

Both for U(III) and U(IV), the situation is more favorable when the electron density from the ligands is near the symmetry axis and away from the basal plane. This requisite coincides whether the dominating parameter is A_2^0 or A_6^0. In a comparison with the lanthanoids, the f-shell electron distribution of U(III) would be similar to Dy(III) (oblate) rather than Er(III) (prolate). Thus, for U(III), ground-state high M_J values are expected when the ligand electronic density is close to the *z*-axis of the molecule, while low M_J values are stabilized by ligand electronic density at or near the basal plane. If the ligands coordinate through lone pair donation, this means that the most favorable situation will be that in which the lone pair is parallel to the basal plane and points toward the main symmetry axis, like in the $Ln(Pc)_2$ case. This favorable situation results in a more axial behavior, with A_2^0 having more weight than A_4^0 or A_6^0, thus desestabilizing the $M_J = \pm 1/2$ state. In a different manner, if the lone pairs bring the effective charge closer to the magic angle, A_2^0would be comparatively weaker, obtaining a magnetism dominated by A_4^0 and A_6^0.

U(III)

Uranium(III) is a f^3 ion, and therefore in the Russell-Saunders scheme it is close to neodymium ($^4I_{9/2}$ level). This has some definite consequences on preferred geometries. For example, a $J = 9/2$ means that fourth-order mixing (tetragonal symmetry) will in most cases facilitate a rapid relaxation of the magnetization. Indeed, molecules with an easy axis will have ground doublets with $M_J = \pm 9/2$ or $M_J = \pm 7/2$, and in both cases a fourth-order mixing implies heavy mixing with $M_J = \pm 1/2$. This means that cubes and triangular dodecahedron are not the best geometries for U(III), and even D_{4d} that is often the most favorable possibility for lanthanoid SIMs can be problematic if it deviates from ideality. In contrast, sixth-order mixing, which is found in trigonal prisms, may often be ideal. If the only extradiagonal parameters are of order six, an Ising $M_J = \pm 9/2$ will only be mixed with $M_J = \mp 3/2$, and in principle this will reduce the quantum tunneling process. Such a trigonal symmetry is particularly robust. Thus, SMM behavior is also favored, even when the ground magnetic doublet has intermediate M_J values, as we have seen in this work.

U(IV)

Uranium(IV) is a f^2 ion, *i.e.* similar to praseodymium, $^3H_4$. This is a rather different situation compared with U(III). In contrast to U(III), this ion is less suitable to provide SIMs as U(IV) has an integer *J* state in which the mixing of the $\pm M_J$ functions through CF operators (of the type O_4^4, O_6^4 and O_6^6) is easier. Thus, depending on the symmetry of the complex, the nature of the ground state will be crucial in determining the SMM properties. For example, tetragonal environments as those provided by bis-phthalocyaninato double-decker complexes, can be adequate for SMM behavior if the ground state is $M_J = \pm 3$. This is so because under such symmetry this ground state can only be contaminated with $M_J = \mp 1$. In turn, if the ground state is $M_J = \pm 4$, a mixing with $M_J = 0$is possible, thus favoring a fast quantum tunneling. Trigonal prisms could also work if the ground state doublet is $M_J = \pm 4$, as in this symmetry it can only be mixed with $M_J = \mp 2$.

Still, the main difference between U(IV) and U(III) lies with the possibility of using U(IV) complexes as spin qubits. In fact, this ion can provide examples with a large tunneling splitting for the ground state. As happens with lanthanoids, uranium complexes with easy-axis ground states $M_J = \pm 4$ or $M_J = \pm 3$, with a fourth-range or with a sixth-range mixing, respectively, will be strongly mixed and therefore will present sizeable tunneling splittings. But because of the much larger ligand-field of actinoids compared with lanthanoids due to the larger size of the 5f orbitals, this mixing, and the corresponding tunneling splitting, will be also much larger than for lanthanoids in favorable cases. In fact, a preliminary, order-of-magnitude calculation assuming a U(IV) complex with the structure of **1** resulted in tunneling splitting which are a full order of magnitude over those recorded for lanthanoids. This expected record-high values for tunneling splitting in U(IV) complexes, in turn can be translated into very long decoherence times.

Concluding remarks

In this paper, we have provided the first theoretical attempt to analyze the magnetic behavior of uranium-based SIMs, which are the next frontier in molecular nanomagnetism. We have found that the theoretical tools that were originally designed for the study of lanthanoid SIMs are essentially valid for uranium SIMs. In particular, by combining a CF model, corrected by the effective charges of the surrounding ligands to account for covalent effects, with the magnetic experimental data, we have

 This journal is © The Royal Society of Chemistry 2013

Published on 22 November 2012 on http://pubs.rsc.org | doi:10.1039/C2SC21490C
Downloaded by Technische Universiteit Delft on 05 February 2013

been able to obtain information on the lowest-lying magnetic levels and the associated wave functions of the nanomagnet. We have shown that these wave functions are compatible with the SMM behavior observed in the five examples of U(III) SIMs reported so far.

Finally, we have proposed some geometrical considerations and practical advices for experimentalists aiming for the rational design of SIMs and qubits based on uranium. In a nutshell, in the right environment, U(III) seems to be an apt choice for the preparation of SIMs, while U(IV) offers an unmatched potential for molecular spin qubits.

Acknowledgements

The present work has been funded by the EU (Project ELFOS and ERC Advanced Grant SPINMOL), the Spanish MINECO (grants MAT2011-22785, MAT2007-61584, and the CONSOLIDER project on Molecular Nanoscience), and the Generalidad Valenciana (Prometeo and ISIC Programmes of excellence). A.G.-A. acknowledges funding by project ELFOS. J.J.B. and S.C.-S. thank the Spanish MECD for FPU predoctoral grants.

Notes and references

1 L. Sorace, C. Benelli and D. Gatteschi, *Chem. Soc. Rev.*, 2011, **40**, 3092.
2 J. D. Rinehart and J. R. Long, *Chem. Sci.*, 2011, **2**, 2078.
3 M. Urdampilleta, S. Klyatskaya, J.-P. Cleuziou, M. Ruben and W. Wernsdorfer, *Nat. Mater.*, 2011, **10**, 502–506.
4 T. Komeda, H. Isshiki, Y. Zhang, N. Lorente, K. Katoh, B. K. Breedlove and M. Yamashita, *Nat. Commun.*, 2011, **2**, 172–178.
5 L. Bogani and W. Wernsdorfer, *Nat. Mater.*, 2008, **7**, 179.
6 M. J. Martínez-Pérez, S. Cardona-Serra, C. Schlegel, F. Moro, P. J. Alonso, H. Prima-García, J. M. Clemente-Juan, M. Evangelisti, A. Gaita-Ariño, J. Sesé, J. van Slageren, E. Coronado and F. Luis, *Phys. Rev. Lett.*, 2012, **108**, 247213.
7 P. C. E. Stamp and A. Gaita-Ariño, *J. Mater. Chem.*, 2009, **19**, 1718.
8 M. N. Leuenberger and D. Loss, *Nature*, 2001, **410**, 789–793.
9 N. Ishikawa, M. Sugita, T. Ishikawa, S. Y. Koshihara and Y. Kaizu, *J. Am. Chem. Soc.*, 2003, **125**, 8694.
10 N. Ishikawa, S. Otsuka and Y. Kaizu, *Angew. Chem., Int. Ed.*, 2005, **44**, 731.
11 N. Ishikawa, Y. Mizuno, S. Takamatsu, T. Ishikawa and S. Y. Koshihara, *Inorg. Chem.*, 2008, **47**, 10217.
12 J. Gómez-Segura, I. Díez-Pérez, N. Ishikawa, M. Nakano, J. Veciana and D. Ruiz-Molina, *Chem. Commun.*, 2006, 2866.
13 (*a*) M. A. AlDamen, J. M. Clemente-Juan, E. Coronado, C. Martí-Gastaldo and A. Gaita-Ariño, *J. Am. Chem. Soc.*, 2008, **27**, 3650; (*b*) M. A. Aldamen, S. Cardona-Serra, J. M. Clemente-Juan, E. Coronado, A. Gaita-Ariño, C. Martí-Gastaldo, F. Luis and O. Montero, *Inorg. Chem.*, 2009, **48**, 3467; (*c*) F. Luis, M. J. Martínez-Pérez, O. Montero, E. Coronado, S. Cardona-Serra, C. Martí-Gastaldo, J. M. Clemente-Juan, J. Sesé, D. Drung and T. Schurig, *Phys. Rev. B: Condens. Matter Mater. Phys.*, 2010, **82**, 060403; (*d*) M. J. Martínez-Pérez, S. Cardona-Serra, C. Schlegel, F. Moro, P. J. Alonso, H. Prima-García, J. M. Clemente-Juan, M. Evangelisti, A. Gaita-Ariño, J. Sesé, J. van Slageren, E. Coronado and F. Luis, *Phys. Rev. Lett.*, 2012, **108**, 247213; (*e*) S. Jiang, B. Wang, H. Sun, Z. Wang and S. Gao, *J. Am. Chem. Soc.*, 2011, **133**, 4730–4733; (*f*) S. Jiang, B. Wang, G. Su, Z. Wang and S. Gao, *Angew. Chem., Int. Ed.*, 2010, **49**, 7448–7451; (*g*) G. Cucinotta, M. Perfetti, J. Luzon, M. Etienne, P. E. Carr, A. Caneschi, G. Calvez, K. Bernot and R. Sessoli, *Angew. Chem.*, 2012, **51**, 1606.
14 Y.-N. Guo, G.-F. Xu, Y. Guoa and J. Tang, *Dalton Trans.*, 2011, **40**, 9953.
15 J. D. Rinehart, K. R. Meihaus and J. R. Long, *J. Am. Chem. Soc.*, 2010, **132**, 7572.
16 Y.-N. Guo, G.-F. Xu, W. Wernsdorfer, L. Ungur, Y. Guo, J. Tang, H.-J. Zhang, L. F. Chibotaru and A. K. Powell, *J. Am. Chem. Soc.*, 2011, **133**, 11948–11951.
17 P.-E. Car, M. Perfetti, M. Mannini, A. Favre, A. Caneschi and R. Sessoli, *Chem. Commun.*, 2011, **47**, 3751.
18 (*a*) J. D. Rinehart, T. D. Harris, S. A. Kozimor, B. M. Bartlett and J. R. Long, *Inorg. Chem.*, 2009, **48**, 3382; N. M. Edelstein and G. H. Lander, in *The Chemistry of the Actinide and Transactinide Elements*, ed. L. R. Morss, N. M. Edelstein and J. Fuger, Springer, Dordrecht, The Netherlands, 3rd edn, 2006, vol. 4, ch. 20; W. W. Lukens and M. D. Walter, *Inorg. Chem.*, 2010, **49**, 4458.
19 N. Magnani, C. Apostolidis, A. Morgenstern, E. Colineau, J. C. Griveau, H. Bolvin, O. Walter and R. Caciuffo, *Angew. Chem., Int. Ed.*, 2011, **50**, 1696.
20 J. D. Rinehart and J. R. Long, *J. Am. Chem. Soc.*, 2009, **131**, 12558.
21 L. Maria, M. P. Campello, A. Domingos, I. Santos and R. J. Andersen, *J. Chem. Soc., Dalton Trans.*, 1999, 2015.
22 J. D. Rinehart, K. R. Meihaus and J. R. Long, *J. Am. Chem. Soc.*, 2010, **132**, 7572.
23 J. D. Rinehart and J. R. Long, *Dalton Trans.*, 2012, **41**, 13572.
24 M. A. Antunes, L. C. J. Pereira, I. C. Santos, M. Mazzanti, J. Marçalo and M. Almeida, *Inorg. Chem.*, 2011, **50**, 9915.
25 J. T. Coutinho, M. A. Antunes, L. C. J. Pereira, H. Bolvin, J. Marçalo, M. Mazzanti and M. Almeida, *Dalton Trans.*, 2012, **41**, 13568.
26 Y. Sun, R. McDonald, J. Takats, V. W. Day and T. A. Eberspacher, *Inorg. Chem.*, 1994, **33**, 4433.
27 N. Magnani, C. Apostolidis, A. Morgenstern, E. Colineau, J. C. Griveau, H. Bolvin, O. Walter and R. Caciuffo, *Angew. Chem., Int. Ed.*, 2011, **50**, 1696.
28 N. Magnani, E. Colineau, R. Eloirdi, J.-C. Griveau, R. Caciuffo, S. M. Cornet, I. May, C. A. Sharrad, D. Collison and R. E. P. Winpenny, *Phys. Rev. Lett.*, 2010, **104**, 197202.
29 D. P. Mills, F. Moro, J. McMaster, J. van Slageren, W. Lewis, A. J. Blake and S. T. Liddle, *Nat. Chem.*, 2011, **3**, 454.
30 J. J. Baldoví, S. Cardona-Serra, J. M. Clemente-Juan, E. Coronado, A. Gaita-Ariño and A. Palii, *Inorg. Chem.*, 2012, **51**, 12565.

Published on 22 November 2012 on http://pubs.rsc.org | doi:10.1039/C2SC21490C
Downloaded by Technische Universiteit Delft on 05 February 2013

31 J. J. Baldoví, S. Cardona-Serra, J. M. Clemente-Juan, E. Coronado, A. Gaita-Ariño and A. Palii, submitted.
32 H. U. Rahman and W. A. Runciman, *J. Phys. Chem. Solids*, 1966, **27**, 1833.
33 H. Nakotte, R. Rajaram, S. Kern, R. J. McQueeney, G. H. Lander and R. A. Robinson, *J. Phys.: Conf. Ser.*, 2010, **251**, 012002.
34 J. J. Baldoví, J. J. Borrás-Almenar, J. M. Clemente-Juan, E. Coronado and A. Gaita-Ariño, *Dalton Trans.*, 2012, **41**, 13705.
35 K. W. H. Stevens, *Proc. Phys. Soc., London, Sect. A*, 1952, **65**, 209.
36 P. Erdös and H. A. Razafimandimby, *J. Phys. Colloques.*, 1979, **40**, C4–171.
37 A. J. Freeman, J. P. Desclaux, G. H. Lander and J. Faber, *Phys. Rev. B*, 1976, **13**, 1168.
38 *The Actinides: Electronic Structure and Related Properties*, ed. A. J. Freeman and J. B. Darby, Jr, Academic, New York, 1974, vol. I, ch. 1; J. Grunzweig-Genossar, M. Kuznietz and F. Friedman, *Phys. Rev.*, 1968, **173**, 562; S. K. Chan and D. J. Lam, *Plutonium and Other Actinides*, ed W. N. Miner, 2009, vol. 1, pp. 19–32.
39 K. T. Moore and G. van der Laan, *Rev. Mod. Phys.*, 2009, **89**, 235.
40 J. Fernández-Rodríguez, S. W. Lovesey and J. A. Blanco, *J. Phys.: Condens. Matter*, 2010, **22**, 022202.
41 S. Alvarez, P. Alemany, D. Casanova, J. Cirera, M. Llunell and D. Avnir, *Coord. Chem. Rev.*, 2005, **249**, 1693.
42 K. R. Meihaus, J. D. Rinehart and J. R. Long, *Inorg. Chem.*, 2011, **50**(17), 8484.
43 C. Apostolidis, A. Morgenstern, J. Rebizant, B. Kanellakopulos, O. Walter, B. Powietzka, M. Karbowiak, H. Reddmann and H.-D. Amberger, *Z. Anorg. Allg. Chem.*, 2010, **636**, 201.

 This journal is © The Royal Society of Chemistry 2013